CrossMark

ORIGINAL PAPER

A nanocomposite consisting of carbon nanotubes and gold nanoparticles in an amphiphilic copolymer for voltammetric determination of dopamine, paracetamol and uric acid

Jingcheng Liu[1] · Yazhen Xie[1] · Kuan Wang[1] · Qingtao Zeng[1] · Ren Liu[1] · Xiaoya Liu[1]

Abstract The amphiphilic copolymer poly(vinylbenzyl thymine-co-styrene-co-maleic anhydride) (PSVM) was synthesized by radical copolymerization of styrene, vinylbenzyl thymine, and maleic anhydride. Its chemical structure was proven by using ^{1}H nuclear magnetic resonance spectroscopy. PSVM was used as a host to prepare a composite consisting of carbon nanotubes and gold nanoparticles by in-situ reduction. The morphology of the nanocomposites was studied by transmission electron microscopy. A glassy carbon electrode coated with this composite is shown to be a viable sensor for the determination of dopamine (DA), paracetamol (PAT) (both at a pH value of 7), and uric acid (UA) (at pH 6). Two linear relationships exists between amperometric current and analyte concentrations. For DA, the linear analytical ranges are from 0.1 to 200 μM and from 200 to 1000 μM. For PAT, the ranges are from 0.1 to 200 μM and from 200 to 1000 μM. For UA, the ranges are from 0.05 to 1000 μM. The respective limits of detection (for S/N = 3) are 56, 27 and 50 nM. The sensor is highly sensitive, stable, reproducible, and selective.

✉ Jingcheng Liu
liujingcheng@jiangnan.edu.cn

[1] The Key Laboratory of Food Colloids and Biotechnology, Ministry of Education, School of Chemical and Material Engineering, Jiangnan University, Wuxi, Jiangsu 214122, China

Introduction

Dopamine (DA) is a crucial neurotransmitter in the brain [1, 2] and reports have indicated that some diseases, such as epilepsy, schizophrenia, and Parkinson's disease, are related to an imbalance in DA concentration [3, 4]. Paracetamol (PAT) is the main component of commonly used analgesics and antipyretics, and is the preferred type of acetanilide drug. However, excess PAT in the human body can cause severe damage to the liver [5]. Uric acid (UA) is the main metabolite of purine metabolism in the body. An imbalance in UA production and excretion caused by metabolism disorders can induce an increase in body fluid acid, thereby affecting the normal operation of cell bodies and increasing the risk of various diseases such as high UA and gout [6, 7]. Therefore, establishing an accurate and sensitive analytical method for detecting DA, PAT, and UA levels is necessary. Methods for detecting DA, PAT, and UA include high-performance liquid chromatography [8], spectrometry [9–12], chemiluminescence [13], capillary electrophoresis [11, 14], and electrochemical sensors [15]. However, most of these methods can be time-consuming and expensive and they involve tedious preprocessing steps [16]. Electrochemical sensors are often the preferred option, providing high selectivity and sensitivity as well as accurate and rapid analysis results, rendering them useful tools for analysis and detection [17].

As a fundamental factor affecting sensing performance, carbon materials, particularly carbon nanotubes (CNT), have

 Springer

attracted considerable attention in the field of electrochemical sensing because they exhibit excellent electrical properties and mechanical strength. Metal nanomaterials can improve the catalytic performance of an electrode by increasing the effective surface area of the sensor, thereby providing a sensitive detection platform for electroactive species [16, 18–20]. Among all metal nanomaterials, Au-based nanomaterials are the most widely used for modifying electrodes because they exhibit high stability and electro catalytic activity as well as excellent conductivity and rapid electron transfer properties [16, 19, 20]. Specifically, CNT–Au nanoparticle composites have been of interest in electrochemical sensor applications for detecting electroactive molecules [21].

In the preparation of CNT–Au composites, the dispersion of CNT in solvents is an obstacle for their further applications due to the poor solubility and processability. Poor dispersion of the CNT in most solvents results from stronger van der Waals attractions between nanotubes than the interaction between the solvent segment and the nanotubes [22]. The destruction of van der Waals attraction becomes possible by addition of the third element capable of preferentially interacting with the nanotubes, which therefore provides electrostatic repulsion or steric repulsion forces to overcome a short range attraction between two nanotubes [23, 24]. Amphiphilic copolymers with hydrophobic-hydrophilic properties are being actively researched to develop functional materials such as composites of polymer–CNT or polymer–Au. Many CNT–Au nanocomposites based on amphiphilic copolymer have been reported [24–26]. On the basis of these observations, it remains a desirable goal to develop efficient strategies for the preparation of CNT/Au nanocomposites through noncovalent assembly.

Poly(styrene-*co*-vinylbenzyl thymine-*co*-maleic anhydride) (PSVM) was synthesized through free radical polymerization and employed to produce a MWCNT/PSVM/Au nanocomposite. The nanocomposites were characterized through transmission electron microscopy (TEM) and subsequently employed to modify a glassy carbon electrode (GCE) to determine DA and PAT (at physiological pH 7) and UA (at physiological pH 6) levels in a phosphate buffer (PB). The experimental results indicated that the modified GCE showed high sensitivity, excellent stability, reproducibility, and selectivity for detecting DA, PAT, and UA. The respective limits of detection were estimated to be as low as 56, 27, and 50 nM (S/N = 3).

Experimental

Chemicals and reagents

Styrene (St), maleic anhydride (MA), and dimethyl sulfoxide (DMSO) (Shanghai Chemical Reagent Co., Ltd., http://www.

sinoreagent.com) were used as received. VBT was synthesized from thymine and vinylbenzyl chloride (Acros Organics, http://acros.lookchem.com), as described previously [27, 28]. Azobisisobutyronitrile (AIBN) (AnalaR, Aladdin, http://www.aladdin-e.com) was recrystallized twice from methanol before use. HAuCl$_4$, NaBH$_4$ (Shanghai Chemical Reagent Co., Ltd., http://www.sinoreagent.com) and multiwalled carbon nanotubes (MWCNTs) (Chengdu Organic Chemicals Institute, Chinese Academy of Sciences, http://timesnano.cnpowder.com.cn) were used as received. The desired pH value of phosphate buffer (0.1 M PB) was obtained by adjusting with 0.1 M K$_2$HPO$_4$ and 0.1 M KH$_2$PO$_4$. DA, PAT and UA (Adamas, Shanghai, China, http://www.adamas-beta.com) were used after dissolving in PB.

Apparatus

The proton nuclear magnetic resonance (^{1}H–NMR) spectrum was recorded using a Bruker Avance Digital 400-MHz spectrometer (Germany, www.bruker.com) with tetramethylsilane as an internal reference in DMSO. TEM images were obtained using a JEM-2100 transmission electron microscope (JEOL, Tokyo, Japan, www.jeol.de/electronopticsen/index.php) with an accelerating voltage of 200 kV. Differential pulse voltammetry (DPV) and a cyclic voltammetry (CV) curves were determined using a Epsilon electrochemical workstation (BAS, USA, www.basvs.com). All voltammetry measurements were carried out at the room temperature.

Synthesis and characterization of PSVM

An amphiphilic copolymer was synthesized through the free radical copolymerization of VBT, St, and MA (Fig. 1). A mixture of St (0.33 g), VBT (0.76 g), and MA (0.61 g) was combined with tetrahydrofuran (THF) to form a co-mono-mer, and AIBN (41 mg) was used as an initiator. The mixtures were stirred for 24 h at 65 °C in N$_2$ atmosphere. The products were dissolved in THF and then poured into excess toluene while undergoing vigorous agitation to produce the copolymers. PSVM was characterized through ^{1}H–NMR spectroscopy.

Preparation of CNT/au nanocomposites

The preparation of CNT/Au nanocomposites involved two steps: the synthesis of an MWCNT/PSVM suspension and preparation of MWCNT/PSVM/Au composites. In a typical process, 20 mg of pristine MWCNT was dispersed into 50 mL of DMSO solution containing 20 mg of PSVM, ultrasonicated for 60 min to obtain a black dispersion solution, and subsequently stirred for an additional 12 h. The suspension was treated through repeated filtration and washing with DMSO

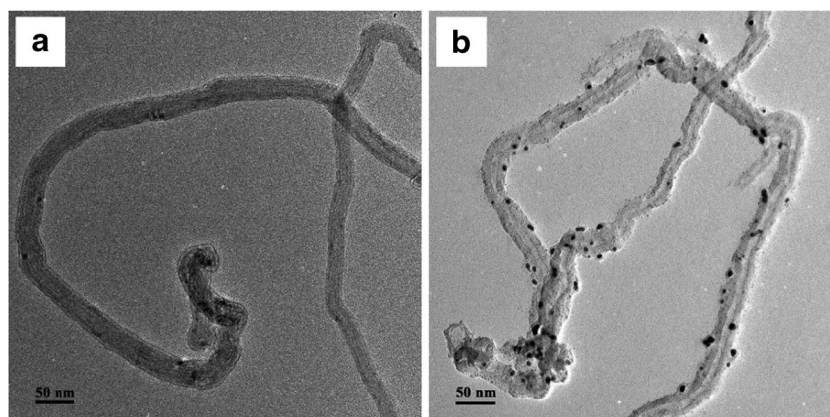**Fig. 1** Synthetic route of amphiphilic copolymer PSVM

to remove unbound PSVM. The resulting MWCNT/PSVM hybrids were irradiated using a 365-nm ultraviolet lamp, and then redispersed in 50 mL of DMSO. Subsequently, 1 mL of $HAuCl_4$ aqueous solution (25 mM) and 7.5 mL of fresh $NaBH_4$ aqueous solution (10 mM) were added to the aforementioned suspension with vigorous stirring at room temperature for 12 h. Finally, the MWCNT/PSVM/Au nanocomposites were collected by three circles of centrifugation (10,000 rpm, 9240 g and 20 min) and washing, and eventually redispersed into 50 mL of DMSO.

Preparation of the electrochemical sensor

The bare GCE was polished to a mirror-like surface by using 0.5 μM of Al_2O_3 powder. The GCE was then rinsed ultrasonically three times with deionized water and ethanol, and then dried in N_2 atmosphere. 6 μL of MWCNT/PSVM/Au dispersion was dropped onto the clean GCE surface and dried in N_2 atmosphere at room temperature. Following this process, the GCE was modified by the MWCNT/PSVM/Au. The resulting sensor was termed a MWCNT/PSVM/Au/GCE sensor and deemed ready for electrochemical measurements. For comparison, an MWCNT/PSVM/GCE sensor was prepared through the same method.

The electrochemical sensing test of the modified GCE was performed using an Epsilon electrochemistry workstation connected to a three-electrode system. With the modified GCE as the working electrode, Pt wire electrode as the counter electrode, and saturated calomel electrode as the reference electrode, CV and DPV curves were plotted.

Results and discussion

Choice of materials

The amphiphilic copolymer PSVM contained St and VBT units, which allowed PSVM to be assembled onto MWCNT sidewalls by π-π stacking interactions, resulting in the formation of MWCNT/PSVM hybrids. In the meantime, VBT units were anchored to the AuNPs surface with N–Au covalent bonds, yielding MWCNT/PSVM/Au nanocomposites. Moreover, VBT can provide hydrogen bonds with the molecules (DA, PAT, UA), which would be favor to improving the detection effect of nanocomposites. Therefore, PSVM not only endowed good dispersion of MWCNTs but also provided a unique environment for the in situ generation of AuNPs and the detection of molecules that can form hydrogen bonds.

^{1}H NMR spectrum of the copolymer PSVM

Polymer structures were characterized by ^{1}H NMR. As shown in Fig. S1, all peaks can be assigned in the VBT and PSVM spectra, indicating PSVM was successfully synthesized (The detailed discussion on ^{1}H NMR was shown in the ESM).

Characterization of MWCNT/PSVM/au nanocomposites

The surface morphologies of the MWCNT/PSVM hybrids and MWCNT/PSVM/Au nanocomposites were characterized through TEM. As displayed in Fig. 2a, the MWCNT/PSVM

Fig. 2 TEM images of **a** MWCNT/PSVM hybrids and **b** MWCNT/PSVM/Au nanocomposite, the mass ratio of $HAuCl_4$ precursors to MWCNTs was 0.1:1

Fig. 3 a DPV curves and **b**
calibration plots recorded with
MWCNT/PSVM/Au/GCE in
pH = 7 PB containing of different
concentrations of dopamine:
0.1 μM–1 mM and paracetamol:
0.1 μM–1 mM. All measurements
were carried out in 0.1 M PB with
scan rate of 20 mV s^{-1}
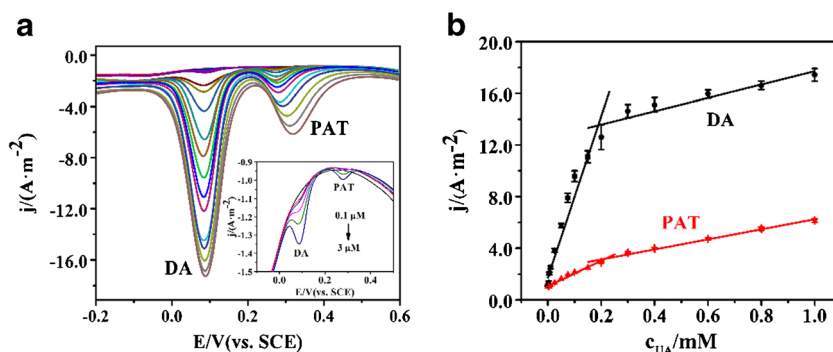
hybrids with cylindrical nanostructures tended to disperse effectively. Aminofunctional MWCNTs were formed through the π–π stacking interactions of MWCNT and PSVM. Fig. 2b displays the cylindrical structure of the MWCNTs, and indicated that the AuNPs were distributed effectively on the surface of the MWCNTs. The aminofunctional MWCNTs were anchored to the in situ synthesized AuNPs surface with N–Au covalent bonds. Thus, AuNPs are strongly tethered to the surface of the MWCNTs. Moreover, PSVM undergo a photodimerization reaction of the pendant thymine units when exposed to 365-nm ultraviolet irradiation. The photodimers created cross-linked networks and wrapped on the MWCNT surface to further improve the stability of MWCNT/PSVM/Au nanocomposites.

Optimization of detection conditions

To achieve the best performance of the determination, the following parameters were optimized: (a) pH value; (b) Au loading; (c) scan rate. Corresponding data and figures are given in the Electronic Supporting Material (ESM) as Fig. S2 and S3. The following experimental conditions were found to give best results: (a) pH value of 7 for DA and PAT, pH value of 6 for UA; (b) with Au loading; (c) scan rate of 20 mV s^{-1}.

Determination of DA, PAT, and UA

DPV generally has superior detection sensitivity and resolution compared with those of other electrochemical

measurement methods [29, 30]. Under optimal conditions, the simultaneous detection of DA and PAT as well as the single detection of UA on the MWCNT/PSVM/Au/GCE sensor was performed using the DPV method. Conventionally, we defined the oxidation current negative. Fig. 3a illustrates the DPV curves of DA and PAT at various concentrations, wherein the concentrations of both species changed simultaneously, causing a linear increase in their peak currents. As displayed in Fig. 3b, the peak current was linearly related to both the DA and PAT concentrations over two ranges: 0.1–200 and 200–1000 μM. The linear equations and correlation coefficient (R^2) were shown in Table 1. The detection limits of DA and PAT were estimated to be 56 and 27 nM (S/N = 3), respectively. The decrease in the slopes for both DA and PAT were assumed to be the result of the slower increase in the DA and PAT peak currents resulting from the adsorption-controlled process being transformed into a diffusion-controlled process at the electrode surface. Similar phenomena have been reported by in previous research [28].

Likewise, as illustrated in Fig. 4(a-b), the peak current increased linearly with the UA concentration increasing, and the regression equation was shown in Table 1. The corresponding limit of detection was calculated to be 50 nM (S/N = 3). All these indicated that the MWCNT/PSVM/Au/GCE sensor exhibited excellent detection performance. As shown in Table 2, MWCNT/PSVM/Au/GCE sensor showed a comparable and even better detection effects compared with other modified electrodes for detecting DA, PAT and UA.

The highly electro catalytic activity of the MWCNT/PSVM/Au/GCE sensor can be attributed to the possibility that

Table 1 The determination effects of MWCNT/PSVM/Au/GCE sensor on DA, PAT and UA

Analyte	Linear range (μM)	Linear regression equation	Correlation coefficient (R^2)	LOD (nM) (S/N = 3)
DA	0.1–200 200–1000	$j(A·m^{-2}) = 62.6\ C(mM) + 1.73$ $j(A·m^{-2}) = 4.39\ C(mM) + 13.2$	0.9850 0.9907	56
PAT	0.1–200 200–1000	$j(A·m^{-2}) = 9.77\ C(mM) + 1.07$ $j(A·m^{-2}) = 3.91\ C(mM) + 2.34$	0.9946 0.9986	27
UA	0.05–1000	$j(A·m^{-2}) = 9.62\ C(mM) + 0.96$	0.9948	50

Fig. 4 a DPV curves and **b** calibration plots recorded with MWCNT/PSVM/Au/GCE in pH = 6 PB containing of different concentrations of uric acid: 0.05 μM–1 mM. All measurements were carried out in 0.1 M PB with scan rate of 20 mV s^{-1}
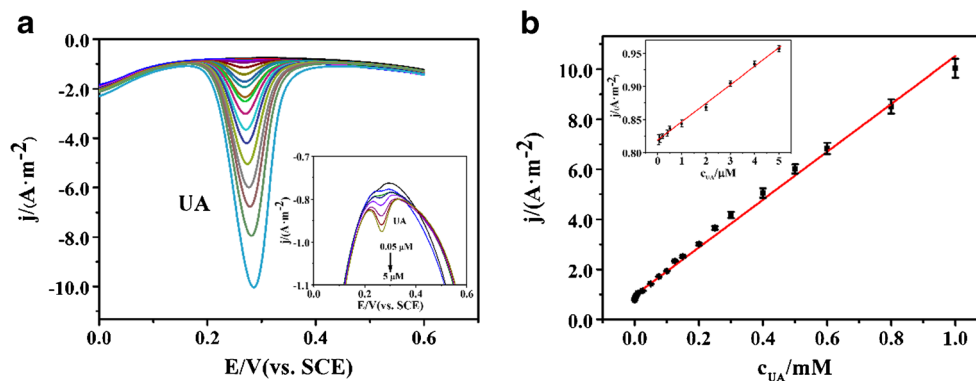
a thymine group in the PSVM interacted with these molecules (DA, PAT and UA) through hydrogen bonds, activating the hydroxyl and amine groups and accelerating the charge transfer kinetics of the molecules on the electrode surface. Furthermore, the electro catalytic effect of the AuNPs and π–interactions between the MWCNTs and the molecules on the electrode surface can promote the charge transfer of DA, PAT, and UA molecules.

Reproducibility, stability, and selectivity

To evaluate the reproducibility of the MWCNT/PSVM/Au/GCE sensor, seven repeated measurements were performed under identical experimental conditions. As illustrated in Fig. S4(a-b), the DPV curves recorded for the 0.1 M PB (pH 7) solution containing a mixture of DA (25 μM) and PAT (25 μM), and the 0.1 M PB (pH 6) solution containing UA (200 μM) demonstrated a relative standard deviation (RSD) of 1.8%, 0.5%, and 0.8% for the DA, PAT, and UA ($n = 7$), respectively, indicating that the MWCNT/PSVM/Au/GCE sensor exhibited excellent reproducibility. The storage stability of the MWCNT/PSVM/Au/GCE sensor was studied by exposing the electrode to air at room temperature and

monitoring the peak current change of DA, PAT, and UA at 3-day intervals over 15 days. As displayed in Fig. S4c, after fifteen days, fewer decreases were observed in the peak current, and the RSDs of DA, PATs and UA ($n = 6$) were 2.8%, 1.6%, and 2.6%, respectively. To study the sensitivity of the sensors, DA, PAT and UA solution containing interfering substances (Fe^{2+}, Ca^{2+}, Li^+, Mg^{2+}, Na^+, K^+, glucose, L-lysine, cysteine, nitrophenol, ascorbic acid, UA or DA/PAT) and the individual components were measured by the MWCNT/PSVM/Au/GCE sensor. As illustrated in Fig. S4d, compared with the species without interference, the average peak current of DA, PAT and UA in the presence of interference remained largely unchanged and average signals change were −4.4%, −3.1%, −3.8%, respectively. It can be clearly seen that the MWCNT/PSVM/Au/GCE sensor exhibited outstanding selectivity for DA and PAT determination.

Real sample analysis

To evaluate the practical application of the MWCNT/PSVM/Au/GCE sensor, serum samples (diluted 100 times with 0.1 M PB, pH = 7) and urine samples (diluted 50 times with 0.1 M PB, pH = 6) consisting of DA, PAT and UA were subjected to

Table 2 Comparison of the analytical performance of the different modified electrodes for determination of DA, PAT and UA

Modified electrode	Linear response range (μM)			Limit of detection (μM)			Reference
	DA	PAT	UA	DA	PAT	UA	
Fe_3O_4@Au /GS-chitosan /GCE	0.5–50	0.4–32	1–90	0.1	0.05	0.2	[8]
(Fc-S-Au/CNC/graphene/GCE	0.40–645	0.62–482	0.90–1440	0.08	0.102	0.128	[16]
SiO_2/MWCNT/func/GC	1.33–4.64	0.67–4.64	0.67–4.64	0.014	0.098	0.068	[31]
PVA/GCE	2–70	-	2–50	1.4	-	0.6	[32]
Chitosan-MWCNT/GC	-	1–145	0.1–18.0	-	0.1	0.016	[33]
Cu(tpa)-EGR	1–50	1–100	-	0.21	0.36	-	[34]
MWCNT-BPVCM-e/GCE	5–1000	5–1000	-	2.3	3.5	-	[35]
MoS_2/PEDOT/GCE	1–80	-	2–25	0.52	-	0.95	[36]
hnp-PtCu/GCE	0.1–1000	-	5–1000	0.1	-	2.3	[37]
MWCNT/PSVM/Au/GCE	0.2–200, 200–1000	0.2–200, 200–1000	0.05–1000	0.056	0.027	0.05	This work

Table 3 Determination of DA, PAT and UA on MWCNT/PSVM/Au/GCE in serum and urine

Sample	Added (μM)			Detected (μM)			Recovery (%)		
	DA	PAT	UA	DA	PAT	UA	DA	PAT	UA
Serum[a]	10	20	50	9.6	19.5	-	96	97.5	-
	20	20	50	19.4	19.8	-	98.5	99	-
	20	10	50	19.7	10.1	-	97	101	-
Urine[b]	-	-	-	-	-	26.3	-	-	-
	50	50	10	-	-	36.6	-	-	103
	50	50	20	-	-	46.8	-	-	102.5
	50	50	40	-	-	66.5	-	-	100.5

[a] bovine serum albumin, diluted 100 times with 0.1 M PB, pH = 7

[b] Human urine, diluted 50 times with 0.1 M PB, pH = 6

a concentration analysis by using a standard addition method. The results were summarized in Table 3 and it was noted that the relative standard deviation (RSD) were within 4.0%. The determination of DA, PAT and UA in serum and urine samples was not interfered with each other. All these indicated that the modified electrode exhibited practical applicability and reliability.

Conclusions

In summary, a MWCNT/PSVM/Au nanocomposite was successfully prepared using a general in situ approach. The nanocomposite was then employed to modify a GCE. This modified GCE can be used for the electrochemical detection of DA and PAT at physiological pH 7 and UA at pH 6 in a wide concentration range. This fabricated sensor also exhibited high sensitivity, excellent stability, reproducibility, and selectivity for detecting DA, PAT, and UA. The sensor is highly reproducible, which may contribute to the development of nanostructured MWCNTs as advanced electrode materials.

Compliance with ethical standards The author(s) declare that they have no competing interests.

References

1. Feng J, Guo H, Li Y, Wang Y, Chen W, Wang A (2013) Single molecular functionalized gold nanoparticles for hydrogen-bonding recognition and colorimetric detection of dopamine with high sensitivity and selectivity. ACS Appl Mater Interfaces 5:1226–1231

2. Sun C, Lee H, Yang J, Wu C (2011) The simultaneous electrochemical detection of ascorbic acid, dopamine, and uric acid using graphene/size-selected Pt nanocomposites. Biosens Bioelectron 26:3450–3455

3. Liu W, Li C, Tang L, Gu Y, Zhang Z (2013a) Facile synthesis of Graphene-poly (styrene sulfonate)-Pt Nanocomposite and its application in Amperometric determination of dopamine. Chin J Anal Chem 41:714–718

4. Su H, Sun B, Chen L, Xu Z, Ai S (2012) Colorimetric sensing of dopamine based on the aggregation of gold nanoparticles induced by copper ions. Anal Methods 4:43981–43986

5. Ramos JVH, de Matos MF, Costa TMH, Dias SLP, Benvenutti EV, de Menezes EW, Arenas LT (2015) Mesoporous chitosan/silica hybrid material applied for development of electrochemical sensor for paracetamol in presence of dopamine. Microporous Mesoporous Mater 217:109–118

6. Qi S, Zhao B, Tang H, Jiang X (2015) Determination of ascorbic acid, dopamine, and uric acid by a novel electrochemical sensor based on pristine grapheme. Electrochim Acta 161:395–402

7. Cardoso AS, Gonzaga NC, Medeiros CC, de Carvalho DF (2013) Association of uric acid levels with components of metabolic syndrome and non-alcoholic fatty liver disease in overweight or obese children and adolescents. J Pediatr 89:412–418

8. Liu M, Chen Q, Lai C, Zhang Y, Deng J, Li H, Yao S (2013b) A double signal amplification platform for ultrasensitive and simultaneous detection of ascorbic acid, dopamine, uric acid and acetaminophen based on a nanocomposite of ferrocene thiolate stabilized Fe3O4@au nanoparticles with graphene sheet. Biosens Bioelectron 48:75–81

9. Vo A, Longoria J, Blackledge W, Yoshii I, Le T, Liou R, Brenner M (2011) Development of a Cobinamide-based cyanide sensor for rapid detection of cyanide toxicity. Chest 150:323A

10. Moini M, Schultz CL, Mahmood H (2003) CE/electrospray ionization-MS analysis of underivatized d/l-amino acids and several small neurotransmitters at attomole levels through the use of 18-crown-6-tetracarboxylic acid as a complexation reagent/background electrolyte. Anal Chem 75:6282–6287

11. Domínguez-Álvarez J, Mateos-Vivas M, García-Gómez D, Rodríguez-Gonzalo E, Carabias-Martínez R (2013) Capillary electrophoresis coupled to mass spectrometry for the determination of anthelmintic benzimidazoles in eggs using a QuEChERS with preconcentration as sample treatment. J Chromatogr A 1278: 166–174

12. Wabaidur SM, Alothman ZA, Naushad M (2012) Determination of dopamine in pharmaceutical formulation using enhanced luminescence from europium complex. Spectrochim Acta A 93:331–334

13. Yuan Y, Han S, Hu L, Parveen S, Xu G (2012) Coreactants of tris (2, 2′-bipyridyl) ruthenium (II) electrogenerated chemiluminescence. Electrochim Acta 82:484–492

14. Wang Y, Xiao L, Cheng M (2011) Determination of phenylureas herbicides in food stuffs based on matrix solid-phase dispersion extraction and capillary electrophoresis with electrochemiluminescence detection. J Chromatogr A 1218:9115–9119

15. Barsan MM, Ghica ME, Brett CMA (2015) Electrochemical sensors and biosensors based on redox polymer/carbon nanotube modified electrodes: a review. Anal Chim Acta 881:1–23

16. Yang L, Huang N, Lu Q, Liu M, Li H, Zhang Y, Yao S (2016) A quadruplet electrochemical platform for ultrasensitive and simultaneous detection of ascorbic acid, dopamine, uric acid and acetaminophen based on a ferrocene derivative functional au NPs/carbon dots nanocomposite and grapheme. Anal Chim Acta 903:69–80

17. Liu W, Li C, Tang L, Tong A, Gu Y, Cai R, Zhang Z (2013c) Nanopore array derived from l-cysteine oxide/gold hybrids: enhanced sensing platform for hydroquinone and catechol determination. Electrochim Acta 88:15–23

18. Devadoss A, Han H, Song T, Kim YP, Paik U (2013) Gold nanoparticle-composite nanofibers for enzymatic electrochemical sensing of hydrogen peroxide. Analyst 138:5025–5030

19. Zhang Y, Liu Y, He J, Pang P, Gao Y, Hu Q (2013) Electrochemical behavior of graphene/Nafion/azure I/au nanoparticles composites modified glass carbon electrode and its application as nonenzymatic hydrogen peroxide sensor. Electrochim Acta 90:550–555

20. Maji SK, Sreejith S, Mandal AK, Ma X, Zhao Y (2014) Immobilizing gold nanoparticles in mesoporous silica covered reduced graphene oxide: a hybrid material for cancer cell detection through hydrogen peroxide sensing. ACS Appl Mater Interfaces 6: 13648–13656

21. Sanghavi BJ, Wolfbeis OS, Hirsch T, Swami NS (2015) Nanomaterial-based electrochemical sensing of neurological drugs and neurotransmitters. Microchim Acta 182:1–41

22. Jiao J, Zhang H, Yu L, Wang X, Wang R (2012) Decorating multi-walled carbon nanotubes with au nanoparticles by amphiphilic ionic liquid self-assembly. Colloids Surface A 408:1–7

23. Kumar NA, Bund A, Cho BG (2009) Novel amino-acid-based polymer/multi-walled carbon nanotube bio-nanocomposites: highly water dispersible carbon nanotubes decorated with gold nanoparticles. Nanotechnology 20:225608–225616

24. Liu J, Lin L, Xie Y, Liu Y, Yuan Y, Liu X, Liu R (2015) An efficient approach to prepare carbon nanotubegold nanoparticles Nanocomposites based on Amphiphilic copolymer containing Coumarin. Chem Lett 44:1497–1499

25. Kang Y, Taton TA (2003) Micelle-encapsulated carbon nanotubes: a route to nanotube composites. J Am Chem Soc 125:5650–5651

26. Kang Y, Taton TA (2005) Core/Shell gold nanoparticles by self-assembly and crosslinking of Micellar, block-copolymer shells. Angew Chem Int Ed 44:409–412

27. Cheng CM, Egbe MI, Grasshoff JM, Guarrera DJ, Pai RP, Warner JC, Taylor LD (1995) Synthesis of 1 -(Vinylbenzyl)thymine, a novel, versatile multi-functional monomer. J Polym Sci Part A: Polym Chem 33:2515–2519

28. Kuo SW, Cheng RS (2009) DNA-like interactions enhance the miscibility of supramolecular polymer blends. Polymer 50:177–188

29. Wang Y, Xiong Y, Qu J, Qu J, Li S (2016) Selective sensing of hydroquinone and catechol based on multiwalled carbon nanotubes/polydopamine/gold nanoparticles composites. Sensor Actuat B-Chem 223:501–508

30. Wang H, Li T, Jia W, Xu H (2006) Highly selective and sensitive determination of dopamine using a Nafion/carbon nanotubes coated poly (3-methylthiophene) modified electrode. Biosens Bioelectron 22:664–669

31. Canevari TC, Raymundo-Pereira PA, Landers R, Benvenutti EV, Machado SA (2013) Sol–gel thin-film based mesoporous silica and carbon nanotubes for the determination of dopamine, uric acid and paracetamol in urine. Talanta 116:726–735

32. Li Y, Lin X (2006) Simultaneous electroanalysis of dopamine, ascorbic acid and uric acid by poly (vinyl alcohol) covalently modified glassy carbon electrode. Sensor Actuat B-Chem 115:134–139

33. Babaei A, Afrasiabi M, Babazadeh M (2010) A glassy carbon electrode modified with multiwalled carbon nanotube/chitosan composite as a new sensor for simultaneous determination of acetaminophen and mefenamic acid in pharmaceutical preparations and biological samples. Electroanalysis 22:1743–1749

34. Wang X, Wang Q, Wang Q, Gao F, Gao F, Yang Y, Guo H (2014) Highly dispersible and stable copper terephthalate metaleorganic frameworkegraphene oxide nanocomposite for an electrochemical sensing application. ACS Appl Mater Interfaces 6:11573–11580

35. Liu R, Zeng X, Liu J, Luo J, Zheng Y, Liu X (2016) A glassy carbon electrode modified with an amphiphilic, electroactive and photosensitive polymer and with multi-walled carbon nanotubes for simultaneous determination of dopamine and paracetamol. Microchim Acta 183:1543–1551

36. Li Y, Lin H, Peng H, Qi R, Luo C (2016) A glassy carbon electrode modified with MoS2 nanosheets and poly (3, 4-ethylenedioxythiophene) for simultaneous electrochemical detection of ascorbic acid, dopamine and uric acid. Microchim Acta 183:2517–2523

37. Zhao D, Fan D, Wang J, Xu C (2015) Hierarchical nanoporous platinum-copper alloy for simultaneous electrochemical determination of ascorbic acid, dopamine, and uric acid. Microchim Acta 182:1345–1352